Modeling the constant-current distance-voltage mode of scanning tunneling spectroscopy

Alex Pronschinske, Daniel J. Mardit, and Daniel B. Dougherty*
Department of Physics, North Carolina State University, Raleigh, North Carolina 27695, USA
(Received 3 June 2011; published 15 November 2011)

We demonstrate the relationship between sample density of electronic states and constant-current distance-voltage spectra starting from the usual expressions for tunneling current in scanning tunneling microscopy experiments. First-order differential equations are derived for the tip position as a function of voltage drop across the tunnel junction for both square and trapezoidal barrier transmission functions. Numerical solutions of the square barrier equation are carried out for different sample density of states and compared with self-consistent integration of the tunneling integral equation. It is shown that normalization of the distance vs voltage spectra by taking logarithmic derivatives reproduces the peak positions in the sample density of states usually to within 0.1 eV. The use of differential equations is proposed as an accurate method for analyzing experimental data and applied to the example case of the π^* orbital of the $c(8 \times 2)$ phase of benzoate on Cu(110).

DOI: 10.1103/PhysRevB.84.205427 PACS number(s): 68.37.Ef

I. INTRODUCTION

The ability to measure local electronic properties at surfaces has been one of the most important outcomes of the invention of the scanning tunneling microscope (STM). Tunneling current in an STM junction depends not only on surface topography but also on the density of electronic states of the tip and the sample. The dependence on density of states makes the STM a tool for revealing structure-function connections at the atomic and nanometer length scale by carrying out scanning tunneling spectroscopy (STS). Scanning tunneling spectroscopy measurements have been used to study surface states on metals[1] and semiconductors,[2] band gaps in semiconductors,[3] molecular orbital-derived states in organic adsorbates,[4] and superconducting gaps.[5,6]

The standard approach to STS was adapted from the revolutionary tunneling studies of Giaever[7] and others that were crucial to the advance of condensed matter physics over the past 50 years. Macroscopic planar tunnel junctions can be created by growing a very thin (1–3 nm) and uniform insulating film between two metallic electrodes. A bias applied over the electrodes results in a measurable tunneling current through the film. The normalized differential tunneling conductance in this experiment has been extensively argued to be proportional to the density of states in the sample.[7–9] At its core, this can be understood as an application of Fermi's golden rule to the scattering of a tunneling electron from one electrode to another.

The analogous STS-based measurement of local electronic structure at a surface involves positioning an STM tip above a feature interest and measuring a local current-voltage (I/V) characteristic at fixed tip height [Fig. 1(a)]. The conceptual connection between local density of states (LDOS) of the sample and the normalized first derivative of the I/V curve is then strongly established by analogy with previous planar tunneling studies. If ρ_S is the sample LDOS, the most common way to express the relationship is:

$$\frac{V}{I}\frac{dI}{dV} \propto \rho_S(eV), \tag{1}$$

where the V/I factor is an empirical normalization that corrects for the exponential background due to the tunneling transmission function.[10] The goal of this paper is to describe the relationship between sample LDOS and a less commonly used method of STS called constant-current distance-voltage spectroscopy, or $z(V)$ spectroscopy for short.

Since the earliest days of STM/STS, it has been recognized that a local measurement of relative tip displacement as a function of voltage [Fig. 1(b)] often exhibits abrupt step-like features related to the high-bias electronic structure in the tunneling junction.[11,12] Initially, $z(V)$ spectroscopy was used to measure barrier resonances in the field emission regime[11] and to relate these resonances to image potential-induced surface states.[12] Later, $z(V)$ measurements were applied to the study of electron and hole polaron levels in polymer and organic films to provide an estimate of transport gaps.[13,14] In recent years, the primary use of $z(V)$ spectroscopy has been to study barrier resonances for the purpose of characterizing local surface potential variations. It has been applied to ultrathin insulating films,[15,16] small organic molecules,[17,18] semiconductors,[19] fullerenes,[20,21] and graphene.[22,23]

The basic $z(V)$ measurement is very simple, as illustrated schematically in Fig. 1(b). An STM tip is positioned over a feature of interest under constant-current feedback control. The voltage across the tunnel junction is then varied, and the tip moves vertically in order to maintain a constant current at the new voltage. If voltage increases, the tip retracts away from the surface to maintain the setpoint current. If voltage decreases, the tip advances toward the surface. Intuitively, the rate of tip motion is proportional to the tunneling probability, so it is expected that a bias regime with an enhanced LDOS will result in an increase in the rate of vertical tip motion.

The major advantage of STS in $z(V)$ mode is that constant-current control allows more gentle probing of surface structures. Small structures can often be strongly perturbed by the injection of tunneling current from an STM tip. In a constant-height [$I(V)$] measurement, the current increases rapidly with voltage, making the probability of tip-induced perturbations increase dramatically. In a $z(V)$ measurement, a small tunneling current can be maintained to minimize this effect and allow STS measurements routinely at higher biases than constant-height mode. This is a very significant advantage for the study of molecular adsorbates which may have important electronic states at high energies and are well

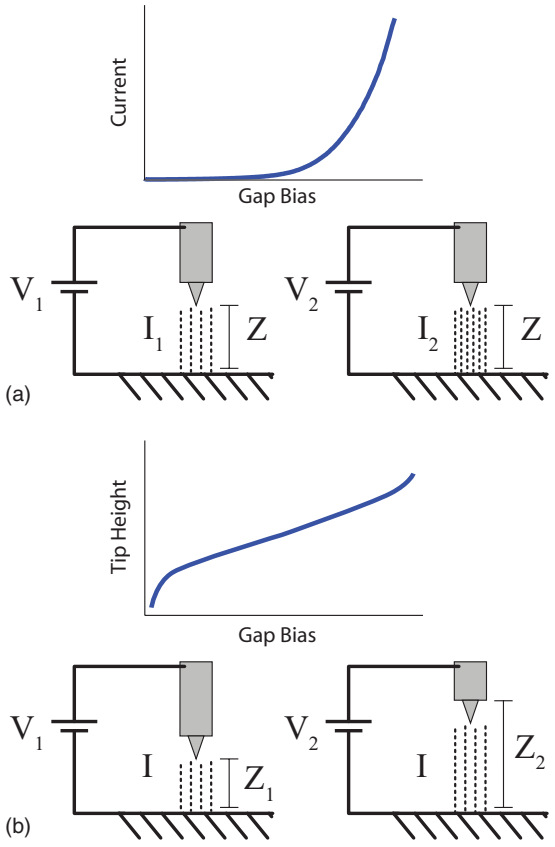

FIG. 1. (Color online) Schematic illustration of (a) constant-height current-voltage and (b) constant-current distance-voltage tunneling spectroscopies.

known to be susceptible to tip-induced chemical reactions,[24,25] diffusion,[26] or desorption.[27,28] Such instabilities are expected to be a general concern for studies of almost any small structure. A possible technical disadvantage of the $z(V)$ technique is that spatial resolution could degrade as the tip moves farther from the surface. However, the total distance moved by the tip is usually small (see results below), and resolution at the scale of single organic molecules has been demonstrated even in the field emission regime.[17]

The most significant drawback to the $z(V)$ method is that its theoretical interpretation has not been made as explicit as the very heavily used constant-height spectroscopy [Eq. (1)]. This was pointed out recently by Ziegler *et al.*[29] who showed experimental evidence that constant-current spectra need to be analyzed with great care. That paper suggested a numerical procedure for extracting density of states information from constant-current spectra that assumed a vanishingly small rate of change of tip position with changing junction voltage. In this paper, we address the detailed connection between density of states and constant-current spectra from a more general theoretical perspective that illustrates the conceptual connection between DOS and $z(V)$ spectra and also allows quantitative analysis of a broad range of experimental data.

This paper is organized as follows. In Sec. II, we will recount the basic tunneling equations as well as recent progress in clarifying the analysis of traditional constant-height measurements. We then derive an ordinary differential equation for tip position as a function of voltage under constant-current conditions for both square and trapezoidal tunneling barriers. In Sec. III, we describe numerical methods for solving this differential equation and characterizing its accuracy. In Sec. IV, we present numerical results followed by discussion of these results in Sec. V, including application to previously published experimental data.

II. TUNNELING EQUATIONS

The starting point for considering most scanning tunneling spectra is the expression for tunneling current that amounts to Fermi's golden rule using a tunneling transmission function calculated in the Wentzels–Kramer–Brillouin (WKB) approximation. For low temperatures where the Fermi functions of both tip and sample are approximately step functions,[30,31] this can be written as:

$$I(z,V) = B\int_0^{eV} \rho_S(E)\rho_T(E-eV)T(z,V,E)dE. \quad (2)$$

In this expression, ρ_S is the LDOS of the sample, ρ_T is the LDOS of the tip, $T(z, V, E)$ is the WKB tunneling transmission function, and $B = (1/2)\,\pi e\hbar^3 m^{-2} A$ with A being the effective tunneling junction area and m the mass of the tunneling electron.[32] We have explicitly indicated in Eq. (2) that I is a function of both z and V. Keeping in mind that z is also a function of V, we find the total derivative of I with respect to V is:

$$dI/dV = \partial_V I(z,V) + \partial_z I(z,V)dz/dV. \quad (3)$$

This expression is a complete relationship between all of the variables relevant to any kind of STS measurement: tunneling current I, junction bias V, and tip height z. To proceed to a more practical form of Eq. (3), the integral expression in Eq. (2) is used to calculate the partial derivatives for specific choices of barrier transmission function $T(z, V, E)$. In this paper, we consider the two most common cases of square and trapezoidal barrier transmission functions. For the square (voltage-dependent) barrier, the transmission function is expressed as:[29–31]

$$T(z,V,E) = \exp\left(-\alpha z\sqrt{\phi + \frac{eV}{2} - E}\right), \quad (4)$$

where $\alpha = 2\sqrt{2m}/\hbar$, z is the distance between tip and sample, ϕ the apparent barrier height of the tunneling junction, and E the energy of the tunneling electron. We substitute this into the integral in Eq. (2) and also make the common assumption that the LDOS of the tip ρ_T is a constant. With these two steps, the partial derivative of I with respect to V can be calculated (being careful to consider the V dependence of the upper integration limit using Leibniz's rule):

$$\partial_V I(z,V) = Be\rho_S(eV)\rho_T(0)T(z,V,eV) + B\int_0^{eV} \rho_S(E)\rho_T\partial_V T(z,V,E)dE. \quad (5)$$

At this point, if we were to assume a constant-height measurement and that the transmission function is approximately constant in the integration range, we would have the usual STS result given by Eq. (1). As noted in several recent works,[30,31]

it is rare that the transmission function will be approximately constant, so the second term should not be neglected as a matter of principle, even for traditional constant-height STS. To proceed, with this term, we evaluate the partial derivative of $T(z, V, E)$ with respect to V:

$$\partial_V T(z,V,E) = -\frac{\alpha e z}{4\sqrt{\phi + \frac{eV}{2} - E}} \exp\left(-\alpha z \sqrt{\phi + \frac{eV}{2} - E}\right). \tag{6}$$

Since the prefactor multiplying the exponential in this expression is slowly varying relative to the exponential, we now approximate it as a constant by evaluating it at the midpoint of the integration interval, $eV/2$, so that it can be factored out of the integral in Eq. (5). This step was first applied by Koslowski *et al.*[30] in their analysis of constant-height STS, though, in their case, it was described (equivalently to our zeroth-order Taylor midpoint expansion) as an application of a well-known generalized mean value theorem for integrals. When the expanded prefactor is removed from the integral, what is left is simply the original integrand for tunneling current that appears in Eq. (2). Thus we can write the partial of I with respect to V as:

$$\partial_V I = Be\rho_S(eV)\rho_T T(z,V,E = eV) - \frac{\alpha e z I}{4\sqrt{\phi}}. \tag{7}$$

Calculating the partial derivative of I with respect z follows precisely the same set of steps except that the only explicit z dependence appears in the exponential of $T(z, V, E)$. The partial of $T(z, V, E)$ with respect to z reads:

$$\partial_z T = \left(-\alpha\sqrt{\phi + \frac{\mathrm{eV}}{2} - E}\right) T. \tag{8}$$

Once again, expanding the slowly varying prefactor to lowest order allows the partial of current with respect to z to be written as:

$$\partial_z I = -\alpha\sqrt{\phi} I. \tag{9}$$

With both partial derivatives in hand, we can substitute into Eq. (3) to find the total derivative of I with respect to V:

$$\frac{dI}{dV} = Be\rho_S(eV)\rho_T T(z,V,eV) - \frac{\alpha e z I}{4\sqrt{\phi}} - \alpha\sqrt{\phi} I \frac{dz}{dV}. \tag{10}$$

However, since we are considering constant-current measurements, ideal electronic feedback will ensure that the total derivative of I vanishes, resulting in the following differential equation for tip position z as a function of voltage V:

$$\alpha\sqrt{\phi} I \frac{dz}{dV} + \frac{\alpha e I}{4\sqrt{\phi}} z - eB\rho_T\rho_S(eV)T(z,V,E = eV) = 0, \tag{11}$$

with $T(z, V, eV)$ given by Eq. (4). This relatively simple expression is analogous to the expression derived by Koslowski *et al.*[30] for dI/dV in constant-height mode STS [see their Eq. (4)]. In addition, it modifies the approach to constant-current STS proposed by Ziegler *et al.*[29] by recognizing that dz/dV cannot vanish in such measurements.

Equations (10) and (11) are the most important results of this paper. They provide an explicit mathematical relationship between a measured $z(V)$ spectrum and the LDOS of a sample. Subsequent sections are devoted to numerical studies of these differential equations as well as discussion of their use in the analysis of experimental STS data. However, the use of a square barrier transmission function can be criticized for consideration of high bias electronic structure where constant-current spectroscopy is most severely needed. Therefore, we will also consider the analog of Eq. (11) derived for the case of a trapezoidal transmission function expressed as:[32]

$$T(z,V,E) = \exp\left\{-\frac{2}{3}\alpha z\left[\frac{(\phi + eV - E)^{3/2} - (\phi - E)^{3/2}}{eV}\right]\right\}. \tag{12}$$

Following similar steps to calculate partial derivatives and approximating the prefactor functions by their midpoint values yields:

$$\alpha f_{1/2} I \frac{dz}{dV} + \alpha f'_{1/2} I z - \frac{3}{2} eB\rho_T\rho_S(eV)T(z,V,E = eV) = 0, \tag{13}$$

where $f_{1/2} = \frac{1}{eV}[(\varphi + eV/2)^{3/2} - (\varphi - eV/2)^{3/2}]$ and $f'_{1/2} - \frac{1}{v}(\frac{3}{2}\sqrt{\varphi + eV/2} - f_{1/2})$.

As described in Sec. IV below, consideration of the more complicated trapezoidal transmission function does not appear to significantly improve the accuracy of a self-consistent integration of Eq. (2). Therefore, numerical study of Eq. (13) is omitted from what follows in favor of focusing attention on the simpler square barrier result, Eq. (11).

III. NUMERICAL METHODS

Numerical integration of the basic tunneling equation [Eq. (2)] was carried out using the MatLab software package's adaptive Gauss–Kronrod quadrature. To simulate constant-current spectra, we numerically integrated Eq. (2) to obtain I, then iteratively adjusted z until we obtained a current equal to the setpoint (I_{set}) within a tolerance of 10^{-16}%. By doing this procedure across a set of different voltage values ($N = 200$), the result is a self-consistent set of simulated $z(V)$ data at a constant current equal to I_{set}. During this process, one can also record the final current values [$I(V)$] at each step to yield a complete set of simulated data similar to what is obtained during real measurements where an $I(V)$ curve from a constant-current mode measurement can be thought of as a way of tracking measurement error.

The differential equation [Eq. (11)] was solved numerically using the method of recursive Taylor coefficients (also known as automatic differentiation),[33] but we also confirmed that a more standard fourth-order Runge–Kutta approach produces the same results. Our numerical solutions of Eq. (11) by this method were also done for 200 points over a given voltage range with the Taylor expansion at each step taken out to 24 terms. In order to obtain an initial value for the differential equation that satisfies Eq. (2), we ran a self-consistent integration at the first voltage point to derive an appropriate starting tip height for the relevant apparent barrier height and tip and sample densities of states.

IV. NUMERICAL RESULTS

A. Numerical integration

As a benchmark for analyzing the differential equations expressed in Eqs. (11) and (13), we directly integrated Eq. (2) for constant-current conditions. This procedure was also used to simulate constant-current STS by Ziegler *et al.*[29] Figure 2 shows a sample LDOS function defined as a flat background (ρ_0) and a single Gaussian peak defined by its height ($\rho_{\max}$), center (E_0), and full-width at half-maximum (w). For our example calculations, we have chosen various physically motivated parameters and display spectra in corresponding physical (nonarbitrary) units. We used an apparent barrier height of 5.0 eV, which is typical for metal surfaces probed with STM tips made from materials like tungsten or Pt-Ir. The simulations used a current setpoint of 10 pA similar to the low currents often used in this form of STS in real experiments. We used a constant 1 $\mathrm{eV}^{-1}\mathrm{nm}^{-3}$ for the tip LDOS and a baseline value of 10^{-3} $\mathrm{eV}^{-1}\mathrm{nm}^{-3}$ for the sample, following the same typical numbers from the seminal work of Tersoff and Hamman.[34] We also approximated the tip by a circular cross-sectional area of radius 1 nm in accordance with the effective areas reported by Pitarke *et al.*[35] It is shown in Fig. 3 that the peaks in the LDOS of the sample translate to peaks in $dz/dV(V)$ with reasonable accuracy. This integration method qualitatively confirms the intuition that peaks in LDOS result in an enhanced rate of vertical tip motion that has been the basis for interpreting previous studies using $z(V)$ spectroscopy.[14,16,20]

In agreement with Ziegler *et al.*,[29] we also find that peaks in the simulated $dz/dV(V)$ spectra tend to be systematically downshifted in energy compared to peaks in the LDOS. The size of the downshift, ΔE, depends on the width and location of the LDOS peak, as illustrated in Fig. 3 for LDOS peaks with widths varying from 0.1 to 1.0 eV. The absolute value of ΔE increases with increasing width of the peak as exhibited by comparison of the $dz/dV(V)$ spectra in Fig. 3(c) with the LDOS functions in Fig. 3(a). For very wide low-energy peaks, the downshift can be as much as 0.35 eV [Fig. 4]. We also note that the peak width is qualitatively transferred from the LDOS to the $dz/dV(V)$ spectrum.

The origin of the systematic downshifts seen in Fig. 4 is the comparable retraction rate due to the LDOS peak and the transmission function background. The closer these rates are to one another, the more distorted peaks in dz/dV will be compared to peaks in LDOS. Much like the case of STS in constant-height dI/dV mode, it is crucial to correct for the transmission function background. We have found that the approach of taking the logarithmic derivative of $z(V)$ [$d(\ln z)/d(\ln V)$] as opposed to the simple derivatives in Fig. 3(c) can correct the distortion due to this background with a high degree of accuracy. The results of this procedure are shown for the case of a square barrier in Fig. 5(a). The offsets ΔE in peak position between the model LDOS and the peaks in the logarithmic derivative of $z(V)$ [i.e. $V/z(dz/dV)$] are typically less than 0.1 eV in almost all experimentally relevant cases, as indicated in Fig. 5(b).

The direct integration method is a brute force way to attack the problem with the advantage that it can be easily and quickly expanded to more complicated transmission functions, such as the trapezoidal barrier function. In Fig. 6, we present the results of self-consistent integration of Eq. (2) using the same example LDOS functions and the trapezoidal barrier approximation. We can see very similar behavior as compared with the use

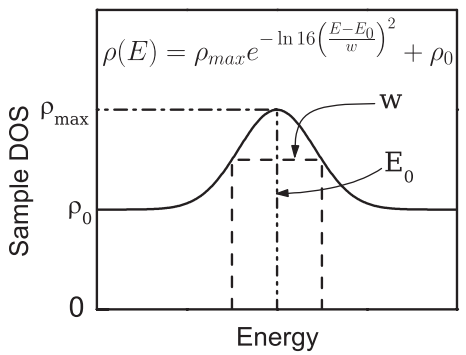

FIG. 2. Gaussian function used for example sample LDOS peaks. Adjustable parameters include peak amplitude ($\rho_{\max}$), baseline (ρ_0), center (E_0), and full-width at half-maximum (w).

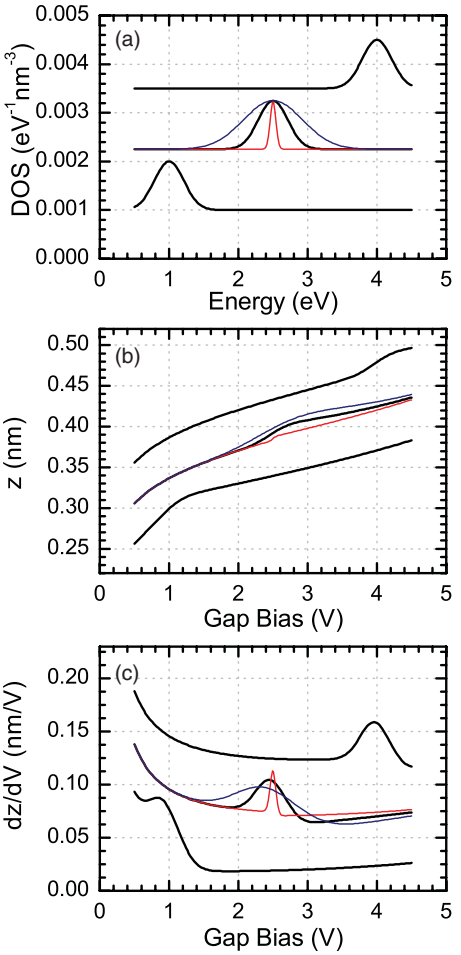

FIG. 3. (Color online) (a) Example LDOS functions with varied centers and widths (E_0 = 1.0, 2.5, and 4.0 eV, and w = 0.1, 0.5, and 1.0 eV). (b) Resulting $z(V)$ curves found by solving the integral tunneling equation [Eq. (2)] with the square barrier transmission function (all middle and top curves are vertically offset for clarity). (c) Numerical derivative of the $z(V)$ curves from part (b).

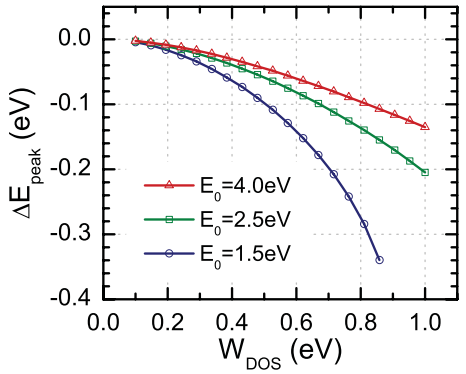

FIG. 4. (Color online) Peak location offsets for $E_0 = 1.5$ eV (blue, circle), 2.5 eV (green, box), and 4.0 eV (red, triangle) as a function of peak width. Peak offset is defined as actual position in LDOS minus position in $dz/dV(V)$ curve. All $dz/dV(V)$ curves are found by solving the integral tunneling equation [Eq. (2)] with the square barrier function.

of the square barrier approximation (Fig. 7). Peak positions in the logarithmic derivative of z with respect to V (to within ~0.1 eV) reflect peak positions in the LDOS. Peak widths are translated accurately, and the monotonic background also has a similar character. Since direct numerical integration shows no significant differences between square and trapezoidal barrier transmission functions, we restrict attention in what follows to the simple square barrier that is most commonly used in theoretical treatments of STS.

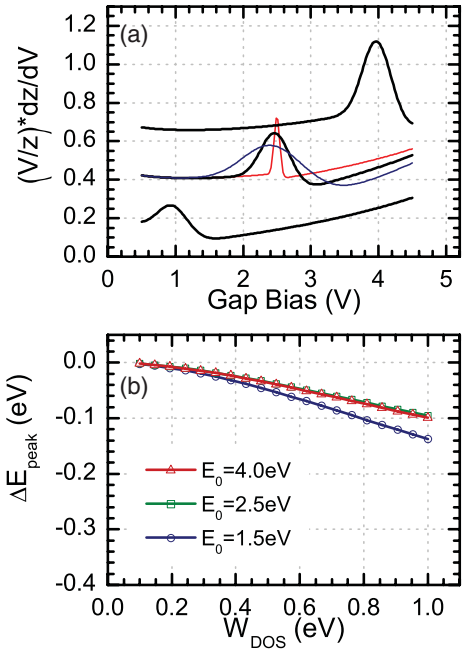

FIG. 5. (Color online) (a) Normalized $dz/dV(V)$ curves for the example LDOS function seen in Fig 3(a). (b) Peak location offsets for $E_0 = 1.5$ eV (blue, circle), 2.5 eV (green, box), and 4.0 eV (red, triangle) as a function of peak width. Peak offset is defined as actual position in LDOS minus position in $(V/z)dz/dV(V)$curve. All $(V/z)dz/dV(V)$ curves are found by solving the integral tunneling equation [Eq. (2)] with the square barrier function.

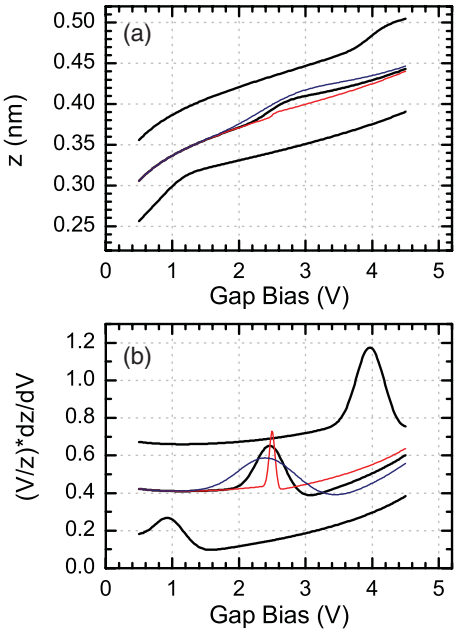

FIG. 6. (Color online) (a) Here, $z(V)$ curves found by solving the integral tunneling equation [Eq. (2)] for LDOS functions in Fig. 3(a) with the trapezoidal barrier transmission function (all middle and top curves are vertically offset for clarity). (b)Logarithmic derivative $[(V/z)dz/dV]$ of the $z(V)$ curves from part (a).

B. Differential equations for a square barrier

From our translation of Eq. (2) into a differential equation [Eq. (11)] for the square barrier transmission function, one can also simulate constant-current STS in an efficient manner using standard numerical methods for first-order differential equations. In addition, Eq. (11) provides a direct analogy for constant-current spectra of the tunneling equations to those used to describe constant-height STS derived by Koslowski *et al.*[30] This is of important conceptual value in defining the spectroscopic information obtained in $z(V)$ spectroscopy.

We solved Eq. (11) for the same model LDOSs considered by numerical integration above. When evaluated over our set

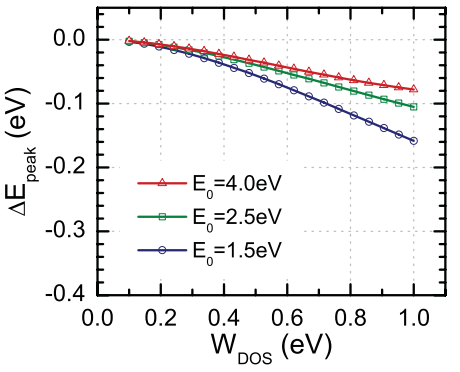

FIG. 7. (Color online) Peak location offsets for $E_0 = 1.5$ eV (blue, circle), 2.5 eV (green, box), and 4.0 eV (red, triangle) as a function of peak width. Peak offset is defined as actual position in LDOS minus position in $(V/z)dz/dV(V)$ curve. All $(V/z)dz/dV(V)$ curves are found by solving the integral tunneling equation [Eq. (2)] with the trapezoidal barrier function.

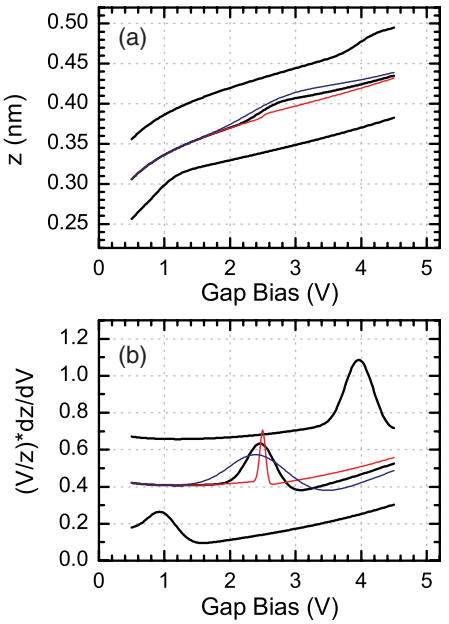

FIG. 8. (Color online) (a) Here, $z(V)$ curves found by solving the differential tunneling equation [Eq. (11)] for LDOS functions in Fig. 3(a) (all middle and top curves are vertically offset for clarity). (b) Logarithmic derivative $[(V/z)dz/dV]$ of the $z(V)$ curves from part (a).

of center and width LDOS peak variations, as seen in Fig. 8, we find this method is comparable to the direct integration. The example $z(V)$ curves obtained by solving the differential equation [Eq. (11)] never vary more than 0.6% from the $z(V)$ curves obtained by self-consistent integration. The small differences in the spectra can be seen as a measure of error for the method and can be attributed to our approximation of the transmission function derivatives and accumulation error from the sequential differential equation solution. Due to the small magnitude of this error, we consider it empirical evidence validating the assumption of slowly varying prefactor functions in Eqs. (6) and (8).

Figure 8 shows that when constant-current distance-voltage spectra are modeled with Eq. (11), it is possible to accurately

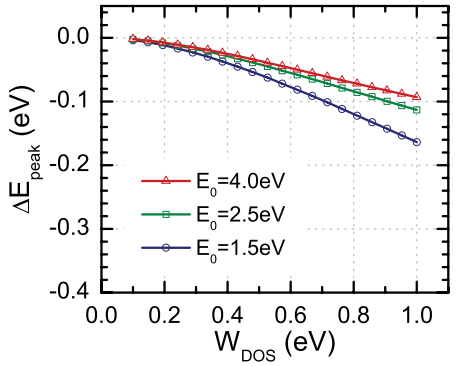

FIG. 9. (Color online) Peak location offsets for $E_0 = 1.5$ eV (blue, circle), 2.5 eV (green, box), and 4.0 eV (red, triangle) as a function of peak width. Peak offset is defined as actual position in LDOS minus position in $(V/z)dz/dV(V)$ curve. All $(V/z)dz/dV(V)$ curves are found by solving the differential tunneling equation [Eq. (11)].

associate peaks in $V/z(dz/dV)$ with peaks in the LDOS. Both peak width and peak position are preserved to good accuracy. In addition, the small systematic downshifts are essentially identical when compared to the self-consistent quadrature solution described above as shown in Fig. 9.

V. DISCUSSION

A. Relating constant-current STS to density of states

The calculations described above establish a clear connection between structure in $z(V)$ measurements and structure in the sample local density of states. This is seen both by direct self-consistent numerical integration of the standard tunneling equation and solution of a corresponding differential equation. Peaks in LDOS translate into peaks in the normalized dz/dV spectra with widths accurately preserved and peak positions preserved up to a systematic correction that is small in many cases. Remarkably, the traditional normalization of dI/dV tunneling spectra has a precise analog that arises empirically from our numerical studies. To a good approximation, we find that:

$$\rho(eV) \propto \frac{V}{z}\frac{dz}{dV}. \tag{14}$$

Calculating the logarithmic derivative of a $z(V)$ spectrum allows determination of peak positions in the LDOS to an accuracy of typically no worse than 0.1 eV. However, this normalization is not perfect, as indicated by Fig. 5, where a small systematic downshift of the peaks in the spectra still exists compared to the model LDOS peak positions. For very high accuracy prediction of expected $z(V)$ spectra from a given density of states, it is necessary to carry out the full solution of Eq. (11). For maximum accuracy extraction of LDOS from experimental $z(V)$ data, it is necessary to use Eq. (11) to directly solve for this quantity, as described in the following section. This will be most important for low-temperature STS experiments, where intrinsic energy resolution may be very high.

B. Application to experimental data

In experiment, constant-current conditions will only be approximate, especially when the sample LDOS changes very rapidly with changing energy near peaks. Equation (11) can be used to solve for the sample LDOS function directly but should be modified to allow for a nonzero dI/dV that must be measured in the experiment in addition to $z(V)$. The resulting equation for sample LDOS using the square barrier transmission function is the following,

$$\rho_S(E) = \frac{2m^2}{\pi e^2\hbar^8 A\rho_t}\left[\frac{dI}{d\mathrm{V}}(V) + \alpha\sqrt{\varphi}I(V)\frac{dz}{d\mathrm{V}}(V) + \frac{e\alpha}{4\sqrt{\varphi}}I(V)z(V)\right]e^{\alpha z(\mathrm{V})\sqrt{\varphi-\frac{eV}{2}}}. \tag{15}$$

The evaluation of this equation requires knowledge of the absolute initial tip position, tip DOS ρ_t, the effective tip area A, as well as the apparent barrier height ϕ. In principle, apparent barrier height could be measured by measuring

the exponential decay constant of tunneling current as a function of relative tip-sample distance. In addition, absolute tip-sample distance can be estimated by controlled crashes of the STM tip with careful monitoring of the total distance the tip moves. In practice, the addition of such delicate measurements to tunneling spectroscopy experiments may not be possible, and these two parameters can be calculated, guessed, or taken as fit parameters. The later approach was used by Ziegler *et al*. in their analysis of constant-current spectra.

The effective tip area and DOS are both very difficult to access experimentally (though proposals for dealing with this problem have been suggested[31,36,37]) and sensitive to uncontrolled tip changes during experiments. This fact, along with the difficulty of reliably measuring both barrier height and absolute tip-sample distance, means that the absolute value of the sample LDOS extracted from $z(V)$ experiments using Eq. (15) is likely to be subject to large uncertainty. However, the shape of the LDOS, including most importantly peak positions, can be extracted reliably.

Figure 10 shows the result of using Eq. (15). Spectra in this figure represent coaverages of 65 constant-current spectra

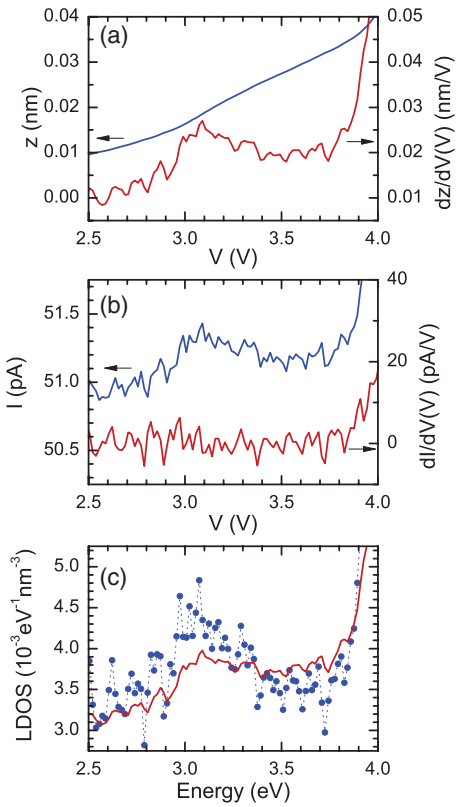

FIG. 10. (Color online) (a) Experimental $z(V)$ spectra ($I = 5$ pA) measured for the $c(8 \times 2)$ phase of benzoate on Cu(110) along with dz/dV obtained by numerical differentiation. Each curve is the result of coaveraging 65 individual spectra followed by smoothing using 2 near neighbor points. (b) Corresponding current and dI/dV data measured simultaneously with the data in part (a). (c) Sample LDOS calculated via Eq. (15) from the data shown in (a) and (b) using $A = 1$ nm, $\varphi = 4.25$ eV, and $z_0 = 0.34$ nm (dotted line with circle markers); also shown is the $(V/z)dz/dV(V)$ curve (solid line) from the same data.

($I_{\text{setpoint}} = 5$ pA) measured over the $c(8 \times 2)$ phase of benzoate on a Cu(110) surface from a previous study.[18] The raw $z(V)$ data show weak structure around $3V$ that is assigned as the π orbital-derived electronic state as described in the ground state DFT calculations of Lennartz *et al*.[38] The bias at which this peak occurs is ideal for the use of $z(V)$ spectroscopy. Numerical extraction of the DOS using Eq. (15) amounts to the removal of a weak background from the dz/dV data.

For the benzoate/Cu(110) data shown here, we estimated an effective tip area of 1 nm, an apparent barrier height of 4.25 eV, and an initial tip-sample distance of 0.34 nm. The initial tip-sample distance was derived from a self-consistent integration of Eq. (2) using the estimated barrier height and the square barrier transmission function. The apparent barrier height was estimated as the mean value between the estimated work function of benzoate/Cu(110) (3.5 eV)[18] and a value typical of tungsten (5.0 eV).[39] All of the $z(V)$ and $I(V)$ curves were smoothed by averaging each point with its two nearest neighbors, differentiated using the central difference method, and after transforming to DOS were all coaveraged together in an effort to reduce noise. The average $z(V)$ and $I(V)$ curves are presented in Figs. 10(a) and 10(b), respectively, along with their first derivatives.

The sample DOS extracted by this method [Fig. 10(c), dash-connected dots] has an improved peak shape as compared to the measured dz/dV curve despite increased noise due to numerical differentiation of the current [Fig. 10(b)]. The close correspondence between dz/dV and DOS is qualitatively expected for a peak with width less than ~0.5 eV centered relatively far from the Fermi level. In this case, systematic offsets are likely to be small (Fig. 4). Conditions where such small offsets will be observable have been demonstrated by Ziegler *et al*. for the case of the relatively low energy LUMO+1 peak of C60 on Ag(111) measured at cryogenic temperatures.[29]

Figure 10(c) also shows the logarithmic derivative of the $z(V)$ data (solid line) from Fig. 10(a). This also agrees with the LDOS extracted from Eq. (15) in peak position and has better signal-to-noise but does not match the peak shape improvements. In order to minimize noise due to numerical differentiation, it would be preferable to carry out measurements, such as those shown in Fig. 9, using two separate lock-in amplifiers to measure dz/dV and dI/dV. Combining these low-noise analog derivatives with measured $z(V)$ and $I(V)$ in Eq. (14) will result in the highest-quality extraction of DOS from experimental data. However, it is worth pointing out that the positions of peaks in the DOS can be read directly from $d(\ln z)/d(\ln V)$ with an accuracy that will usually be better than 0.1 eV.

VI. SUMMARY AND CONCLUSIONS

In summary, we have illustrated a quantitative relationship between sample local density of states and constant-current distance-voltage spectra measured with an STM tip. Direct integration of the tunneling equations shows that peaks in the LDOS translate into peaks in the first derivative of relative tip displacement as a function of tip-sample voltage for both square and trapezoidal tunneling barrier transmission functions. This is also true for solutions of a conceptually

simpler differential equation derived from integral expression for tunneling current. Our numerical results show that normalizing $z(V)$ spectra by taking a logarithmic derivative does a very good job of removing most distortions due to the transmission function background. Furthermore, the differential equation [Eq. (10)] provides a straightforward and accurate means of extracting sample LDOS from constant-current tunneling spectra without need for empirical normalization strategies.

These results establish a strong basis for the interpretation of peaks in tunneling spectra measured in constant-current mode. This technique has great advantages in that it allows tunneling spectroscopy to be carried out on physical systems that may be sensitive to high-current densities injected from an STM. The use of small constant currents in tunneling spectra is expected to allow increasingly routine spectroscopic studies of nanoscale systems, including single molecules, molecular assemblies, and nanostructured surfaces.

*Corresponding author: dbdoughe@ncsu.edu

[1]M. F. Crommie, C. P. Lutz, and D. M. Eigler, Nature **363**, 524 (1993).
[2]R. J. Hamers, R. M. Tromp, and J. E. Demuth, Phys. Rev. Lett. **56**, 1972 (1986).
[3]R. M. Feenstra, V. Ramachandran, and H. Chen, Appl. Phys. A-Mater. Sci. Process. **72**, S193 (2001).
[4]K. W. Hipps, D. E. Barlow, and U. Mazur, J. Phys. Chem. B **104**, 2444 (2000).
[5]D. Eom, S. Qin, M. Y. Chou, and C. K. Shih, Phys. Rev. Lett. **96**, 027005 (2006).
[6]E. W. Hudson, S. H. Pan, A. K. Gupta, K. W. Ng, and J. C. Davis, Science **285**, 88 (1999).
[7]I. Giaever, Phys. Rev. Lett. **5**, 147 (1960).
[8]J. Bardeen, Phys. Rev. Lett. **6**, 57 (1961).
[9]J. R. Schrieffer, Rev. Mod. Phys. **36**, 200 (1964).
[10]J. A. Stroscio, R. M. Feenstra, and A. P. Fein, Phys. Rev. Lett. **57**, 2579 (1986).
[11]R. S. Becker, J. A. Golovchenko, and B. S. Swartzentruber, Phys. Rev. Lett. **55**, 987 (1985).
[12]G. Binnig, K. H. Frank, H. Fuchs, N. Garcia, B. Reihl, H. Rohrer, F. Salvan, and A. R. Williams, Phys. Rev. Lett. **55**, 991 (1985).
[13]S. F. Alvarado, P. F. Seidler, D. G. Lidzey, and D. D. C. Bradley, Phys. Rev. Lett. **81**, 1082 (1998).
[14]D. B. Dougherty, W. Jin, W. G. Cullen, G. Dutton, J. E. Reutt-Robey, and S. W. Robey, Phys. Rev. B **77**, 073414 (2008).
[15]E. D. L. Rienks, N. Nilius, H. P. Rust, and H. J. Freund, Phys. Rev. B **71**, 241404 (2005).
[16]C. D. Ruggiero, T. Choi, and J. A. Gupta, Appl. Phys. Lett. **91**, 253106 (2007).
[17]D. B. Dougherty, P. Maksymovych, J. Lee, and J. T. Yates, Phys. Rev. Lett. **97**, 236806 (2006).
[18]A. Pronschinske and D. B. Dougherty, J. Phys. Chem. Lett. **1**, 2613 (2010).
[19]J. A. Kubby and W. J. Greene, Phys. Rev. Lett. **68**, 329 (1992).
[20]M. Feng, J. Zhao, and H. Petek, Science **320**, 359 (2008).
[21]J. Zhao, M. Feng, J. L. Yang, and H. Petek, ACS Nano **3**, 853 (2009).
[22]S. Bose, V. M. Silkin, R. Ohmann, I. Brihuega, L. Vitali, C. H. Michaelis, P. Mallet, J. Y. Veuillen, M. A. Schneider, E. V. Chulkov, P. M. Echenique, and Klaus Kern, New J. Phys. **12**, 023028 (2010).
[23]A. Sandin, A. Pronschinske, J. E. Rowe, and D. B. Dougherty, Appl. Phys. Lett. **97**, 113104 (2010).
[24]S. W. Hla and K. H. Rieder, Annu. Rev. Phys. Chem. **54**, 307 (2003).
[25]W. Ho, J. Chem. Phys. **117**, 11033 (2002).
[26]M. Bohringer, W. D. Schneider, and R. Berndt, Surf. Sci. **408**, 72 (1998).
[27]S. Alavi, R. Rousseau, G. P. Lopinski, R. A. Wolkow, and T. Seideman, Faraday Discuss. **117**, 213 (2000).
[28]P. Kruse and R. A. Wolkow, Appl. Phys. Lett. **81**, 4422 (2002).
[29]M. Ziegler, N. Neel, A. Sperl, J. Kroger, and R. Berndt, Phys. Rev. B **80**, 125402 (2009).
[30]B. Koslowski, C. Dietrich, A. Tschetschetkin, and P. Ziemann, Phys. Rev. B **75**, 035421 (2007).
[31]M. Passoni, F. Donati, A. L. Bassi, C. S. Casari, and C. E. Bottani, Phys. Rev. B **79**, 045404 (2009).
[32]C. Wagner, R. Franke, and T. Fritz, Phys. Rev. B **75**, 235432 (2007).
[33]A. Asaithambi, Appl. Math. Comput. **215**, 4400.
[34]J. Tersoff and D. R. Hamann, Phys. Rev. Lett. **50**, 1998 (1983).
[35]J. M. Pitarke, F. Flores, and P. M. Echenique, Surf. Sci. **234**, 1 (1990).
[36]B. Koslowski, H. Pfeifer, and P. Ziemann, Phys. Rev. B **80**, 165419 (2009).
[37]B. Naydenov and J. J. Boland, Phys. Rev. B **82**, 245411 (2010).
[38]M. C. Lennartz, N. Atodiresei, L. Müller-Meskamp, S. Karthäuser, R. Waser, and S. Blügel, Langmuir **25**, 856 (2008).
[39]A. G. Fedorus and A. G. Naumovets, Surf. Sci. **21**, 426 (1970).